Structure tuning by Fermi-surface shifts in low-dimensional systems



2002 J. Phys.: Condens. Matter 14 4199

(http://iopscience.iop.org/0953-8984/14/16/311)

INSTITUTE OF PHYSICS PUBLISHING JOURNAL OF PHYSICS: CONDENSED MATTER

J. Phys.: Condens. Matter **14** (2002) 4199–4209 PII: S0953-8984(02)29090-6

# Structure tuning by Fermi-surface shifts in low-dimensional systems

**C Deisl, K Swamy, R Beer, A Menzel and E Bertel**

Institute of Physical Chemistry, University of Innsbruck, A-6020 Innsbruck, Austria

Received 17 January 2002, in final form 25 February 2002
Published 11 April 2002
Online at stacks.iop.org/JPhysCM/14/4199

**Abstract**

In low-dimensional systems, electron–electron correlation as well as electron–phonon coupling is enhanced. This tends to link the geometry to the Fermi-surface position, for instance via formation of charge-density waves. The quasi-one-dimensional c(2 × 2)-Br/Pt(110) surface system is used here to explore this effect. NO adsorption gives rise to a considerable Fermi-surface shift and causes the system to go through a succession of complex phases comprising commensurate, long-range-ordered structures, as well as periodic and chaotic soliton lattices. The structural evolution is in qualitative agreement with the predictions of the discrete Frenkel–Kontorova model.

(Some figures in this article are in colour only in the electronic version)

## 1. Introduction

There is an intimate relationship between the electronic and geometric structure of solids. Metal–insulator transitions in group IIa elements under pressure and different magnetic phases in strained transition metal films are just two examples of a change in electronic structure induced by geometry parameter variation. It is very difficult, however, to significantly influence the geometry of three-dimensional (3D) solids by manipulating their electronic structure. If the dimensionality is lowered, electronic correlation effects and the electron–phonon coupling are enhanced. Consequently, the geometry becomes less robust with respect to subtle changes in the electronic structure. This renders 2D and 1D solids interesting objects for the study of electronically driven phase transitions. Depending on the delicate balance between electron–phonon coupling, electron–electron interaction and (anisotropic) bandwidth there are a multitude of phases observed in low-dimensional compounds ranging from normal metallic to (Mott) insulating and superconducting, on the one hand, and from different magnetically ordered phases (spin–Peierls, antiferromagnetic, spin-density-wave (SDW)) to charge-ordered phases ($2k_F$ and $4k_F$ charge-density waves (CDW)), on the other hand. The possibility of influencing this balance by making relatively minor changes of the electronic properties poses an interesting challenge and makes low-dimensional systems an attractive arena for materials design [1, 2].

0953-8984/02/164199+11$30.00  

A quasi-one-dimensional (1D) surface system has the particular advantage of being accessible to (reversible) manipulation as well as direct observation at the same time, thus making feasible detailed studies of the induced phase transitions. Prominent examples of quasi-1D surface structures are metal deposits on Ge(111) and Si(111) surfaces [3]. Plummer and co-workers [4] observed a phase transition in Pb/Ge(111), which they attributed to a surface CDW although this particular system exhibits no quasi-1D behaviour. This group also proposed deliberately shifting the Fermi wavevector in a surface CDW system by adatom deposition in order to tune the periodicity of the ad-layer structure. This is an intriguing proposal, but it is difficult to realize. First, for a continuous tuning of periodicities the surface defect concentration is crucial, because defects tend to act as pinning centres. Semiconductor surfaces exhibit an inherently large defect concentration which tends to interfere with a Fermi-level-controlled self-structuring mechanism [5]. It seems therefore advisable to look for a quasi-1D electronic system on a metal surface, which can be prepared with a low defect density. A natural choice is fcc(110) surfaces, because they provide an inherently large anisotropy. The question then is, whether electrons can be sufficiently confined on a metal surface to exhibit correlations large enough for spontaneous symmetry-breaking phase transitions to occur. Even if a surface system can be devised with strong electron confinement into one dimension, the screening provided by the substrate Fermi sea could eventually be strong enough to quench the phase transitions that we are interested in. In the present study we investigate the adsorption system c(2 × 2)-Br/Pt(110) [6, 7], which shows clear signs of quasi-1D behaviour, including a phase transition into a (3 × 1) structure, which we assign to the formation of a CDW [8]. Angle-resolved ultraviolet photoemission spectroscopy (ARUPS) peak shapes of bands near their crossing with the Fermi level reveal many-body effects [9] indicating strong electron–electron correlation in addition to the electron–phonon coupling signalled by the appearance of a CDW ground state. As, in addition, the c(2 × 2)-Br/Pt(110) ad-layer is stable up to a temperature of ∼780 K this surface is a suitable candidate for 'Fermi-surface engineering'. The quasi-1D behaviour of the c(2 × 2)-Br/Pt(110) ad-layer is actually due to the formation of Pt–Br chains in $[1\bar{1}0]$ direction. In contrast to our original assignment based solely on STM data [8], these chains are not formed by substitutional insertion of Br into the close-packed Pt rows. Rather, they consist of close-packed Pt atom rows with the Br riding on every second short-bridge site [7]. As the missing-row reconstruction of the clean Pt surface is lifted during the preparation of the c(2 × 2) Br/Pt ad-layer, the distance between neighbouring Pt–Br chains equals the Pt lattice constant (3.92 Å).

The occurrence of a CDW is not a necessary condition for the Fermi-surface-dependent tuning of ad-layer periodicities. $2k_F$-interactions within the ad-layer can be conveyed by Friedel oscillations without the concomitant occurrence of a zero-energy phonon mode. Usually this is not observed, however, because Friedel oscillations on a metal surface tend to fall off rather quickly (as $1/r^5$ for bulk states on a surface or as $1/r^3$ for surface states [10]). Furthermore, the contribution of surface states to the total charge density on a metal surface is normally not large enough to impose a long-range ordering onto the ad-layer. In quasi-1D surface layers, however, Friedel oscillations are expected to exhibit a rather slow fall-off ($1/r$ dependence [11]). If in addition the density of states at $E_F$ is large, as could be the case for a d-derived surface state, the adsorbate interaction may become long range and strong enough to impose Fermi-surface-dependent periodicities even at moderate adsorbate coverages. It should be noted that the conditions of low dimensionality and high density of states at $E_F$ are exactly what is required for a strong electron–phonon coupling. Hence, even if such a system remains in the normal state, it will be at least very close to a CDW instability.

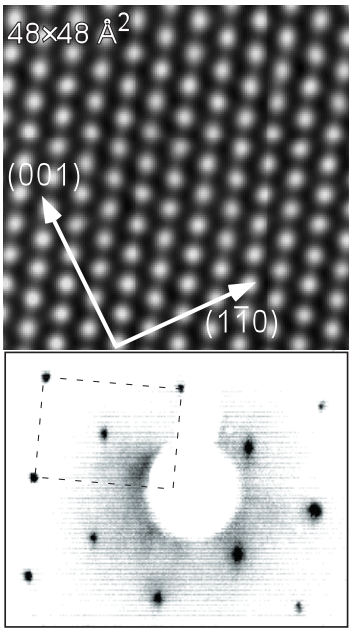


**Figure 1.** An STM image (top) and LEED pattern (bottom) of the c(2 × 2)-Br/Pt(110) adsorption system. The dashed rectangle in the LEED pattern marks a (1 × 1) unit cell.

## 2. Experimental details

Cleaning of the Pt(110) surface was performed by cycles of Ar sputtering and heating in oxygen to remove C impurities. The last stage of cleaning prior to Br adsorption consisted of two cycles of low-temperature oxygen adsorption and subsequent desorption. This ensured that no traces of $CO_2$ could be detected in the temperature-programmed desorption (TPD) spectra (a criterion which proved to be much more sensitive to C contamination than Auger electron spectroscopy). Br was dosed onto the surface by means of a solid-state electrolysis cell. The Br coverage was determined from TPD spectra and low-energy electron diffraction (LEED) using the c(2 × 2)-Br/Pt(110) structure as a calibration point for $\Theta_{Br} = 0.5$ ML (monolayers). LEED patterns were recorded using a highly sensitive CCD camera. The c(2 × 2) structure was prepared by adsorption of a few ML of Br and subsequent heating to 780 K. This caused all Br in excess of $\Theta_{Br} = 0.5$ ML to desorb and yielded a well-developed c(2 × 2) pattern with large terraces [8, 12] (figure 1). Scanning tunnelling microscopy (STM) was carried out at room temperature. In order to induce a Fermi-surface shift, CO and NO were used. Both adsorb rather weakly on the c(2 × 2)-Br/Pt(110) surface [13]. This is desirable in order to avoid a local reconstruction due to direct bond formation of these co-adsorbates. Nevertheless they do induce a Fermi-surface shift in the surface state as detected in ARUPS and demonstrated in figure 2. Figure 2 shows the NO-induced shift of the surface-state band producing the Fermi surface responsible for the CDW formation [8]. The shift was determined from electron distribution curves (EDCs) recorded by ARUPS with an angular resolution of $\pm 1^\circ$ and an energy resolution of 50 meV. Relative molecular coverages of CO and NO were determined from integration of TPD spectra recorded with a heating rate of 3 K $s^{-1}$ [13]. Comparison with STM images, where both molecules are imaged as depressions, then yielded an absolute calibration. Saturation at 300 K was found to be at $\Theta_{NO\,(CO)} = 0.25$ ML. By the same token, saturation at 100 K occurred at $\Theta_{NO\,(CO)} = 1$ ML.

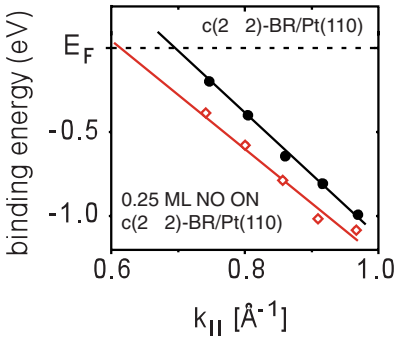


**Figure 2.** The Fermi-surface shift obtained upon adsorption of 0.25 ML of NO. Symbols mark the peak positions in the corresponding energy distribution curves; the solid lines represent their linear extrapolation to the Fermi level.

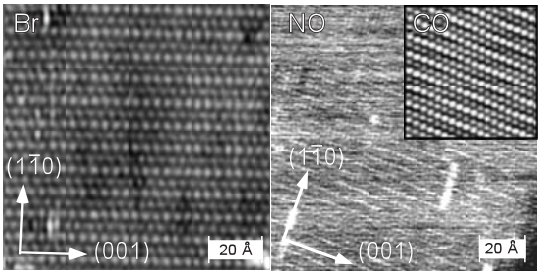


**Figure 3.** STM images comparing the (3 × 1) structure obtained by adsorption of additional Br (left) and NO (right) onto the c(2 × 2)-Br/Pt(110) surface. The inset shows the (3 × 1) structure obtained upon CO adsorption. Although the quality of the STM image for NO adsorption is low due to unstable tip conditions, LEED $I(E)$ curves confirm the basic similarity of the (3 × 1) structures for all three cases.

## 3. Results

Adsorption of small traces (∼2% of a ML) of CO or NO onto the c(2 × 2)-Br/Pt(110) surface causes a transition into a global (3 × 1) structure, which we assign to a CDW phase just as in the case of additional Br exposure [8]. Figure 3 shows a comparison of the two structures as imaged by STM. This and the LEED $I(E)$ curves for the Br-induced ($\Theta_{\mathrm{Br}}^{excess} \approx 0.14$ ML) and the NO-induced ($\Theta_{\mathrm{NO}} \approx 0.05$ ML) (3 × 1) structures clearly indicate that the two structures are essentially identical with respect to the Br positions. The NO (CO) molecules are not detected in the STM images at these low coverages, presumably because they are too mobile at room temperature. Further NO exposure results in a fluid phase [14] featuring anti-phase (3 × 1) domains separated from each other by poorly ordered zigzag chains of NO (figure 4(*a*)). While the zigzag arrangement of molecules prevails within the rows, a linear configuration occurs as well and at room temperature the molecules are actually seen to hop between different configurations on a timescale of a few seconds. This leads to a statistical distribution of occupied sites within the zigzag chains. Therefore the LEED pattern of all the adsorbate structures discussed below, which contain such zigzag chains as building blocks, exhibits a ($n$ × 1) structure rather than an ($n$ × 2) structure, which one would expect for a periodic pattern of well-ordered zigzag chains. The structure shown in figure 4(*a*) was analysed in more detail in [13] and [14]. Figure 4(*b*) shows the STM image obtained at a coverage of $\Theta_{\mathrm{NO}} = 0.11$ ML. Here, the zigzag rows exhibit long-range ordering with a periodicity of seven

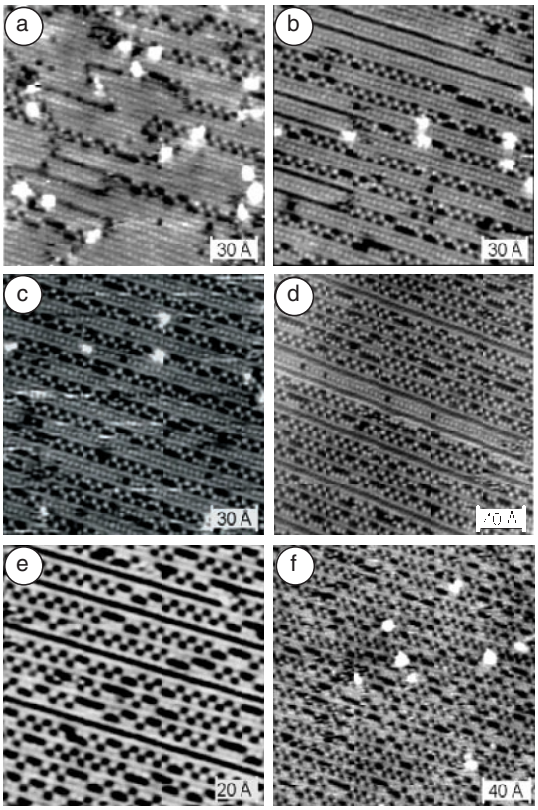


**Figure 4.** A series of STM images showing the structural evolution of the NO/Br/Pt(110) surface as the NO coverage is gradually increased ((*a*) 0.07 ML, (*b*) 0.11 ML, (*c*) 0.14 ML, (*d*) 0.19 ML, (*e*) 0.23 ML, (*f*) 0.25 ML).

nearest-neighbour (nn) intervals ($7 \times 2.77$ Å $= 19.4$ Å). Such a long-range ordering cannot be attributed to direct adsorbate–adsorbate interaction. The only forces having a sufficient range to account for such a pattern are either of elastic [15] or electronic origin. In the present case the close correlation of the observed periodicities with the Fermi-surface position, which will be demonstrated further below, argues strongly in favour of an electronic effect. Between the zigzag rows, small domains of the $(3 \times 1)$ structure are observed. These domains are anti-phase domains, because the zigzag rows introduce a phase shift of $2\pi/3$ between neighbouring $(3 \times 1)$ domains. At 0.11 ML the NO coverage is not yet sufficient to have the surface completely covered with zigzag chains in sevenfold periodicity. Thus, some chains end within the terrace. As the domains above and below a zigzag chain are not in phase, they cannot be smoothly joined at the end of such an NO row. Instead, two phase discommensurations are observed to emerge from the NO rows, each of which introduces a phase change of $\pi/3$. Such phase discommensurations between two CDW domains are also called solitons [16]. In the STM images they appear as straight, dark lines. From a comparison with the coverage measured by TPD and in view of their corrugation, which differs from the one measured at NO positions, we conclude that these solitons are not associated with adsorbed NO and call them 'bare' solitons. Thus, bare solitons introduce a phase shift of $\pi/3$, while the NO zigzag rows can be considered as 'dressed' solitons causing a phase shift of $2\pi/3$. The end of a zigzag row constitutes a vortex, joining three $(3 \times 1)$ domains with three different phases. Figure 5 provides a detailed view

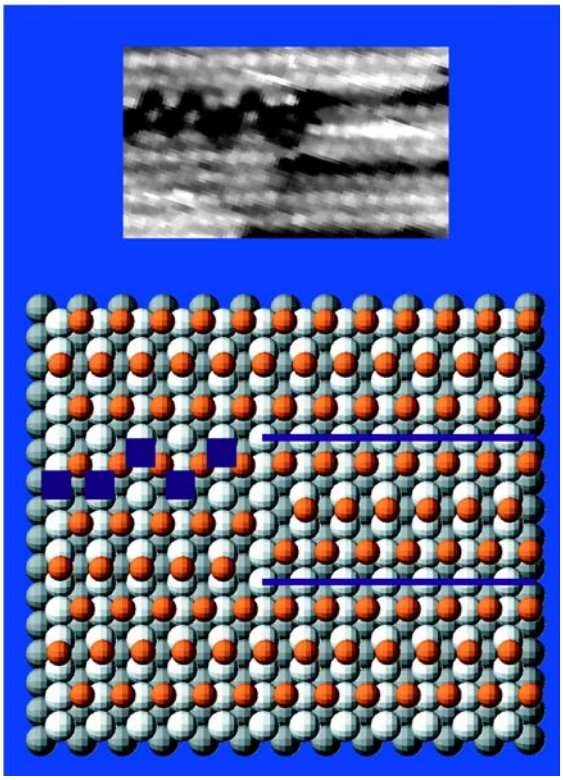

**Figure 5.** An STM image and a ball model of a vortex observed in figures 4(*a*) and (*b*). In the ball model, Pt atoms are grey, Br atoms red and the dark blue squares symbolize the NO molecules. The dark blue lines indicate the position of the bare solitons continuing the dressed soliton.

and a ball model of such a vortex, where two bare solitons emerge from a dressed soliton. The model is inspired by LEED $I(E)$ analysis and *ab initio* total-energy calculations of the c(2 × 2)-Br/Pt(110) [7] and the (3 × 1)-Br/Pt(110) structures, showing that Br occupies short-bridge sites in the former and short-bridge as well as long-bridge sites in the latter structure. It is constructed in such a way that within the dressed soliton the Br adatoms form a local (2 × 1) structure. This choice is not unique. Alternatively, one could construct a model yielding a local c(2 × 2) geometry within the range of the zigzag rows. The observed room temperature mobility of the molecules, however, is more easily accounted for in the (2 × 1) model. Previous experiments as well as the calculations show that within the pure Br ad-layer the (2 × 1) and the c(2 × 2) geometry have almost the same energy.

In figure 4(*c*), the NO coverage is increased to 0.14 ML. This is sufficient for NO zigzag rows to form a (7 × 1) structure completely covering the surface with only little disorder and without intervening bare solitons. Further NO exposure to $\Theta_{NO} = 0.19$ ML (figure 4(*d*)) causes a reappearance of bare solitons and a dramatic reduction of (3 × 1) domains in favour of more tightly packed molecule chains arranged in domains with local fourfold periodicity. At $\Theta_{NO} = 0.23$ ML (figure 4(*e*)) the (3 × 1) domains have completely disappeared and the overlayer structure consists entirely of (4 × 1) domains with intervening bare solitons in an irregular succession. At $\Theta_{NO} = 0.25$ ML (figure 4(*f*)), finally, the bare solitons are gone again and a long-range-ordered (4 × 1) domain is observed (as mentioned above, the order is well developed in the $(1\bar{1}0)$ direction but randomly perturbed in the (001) direction).

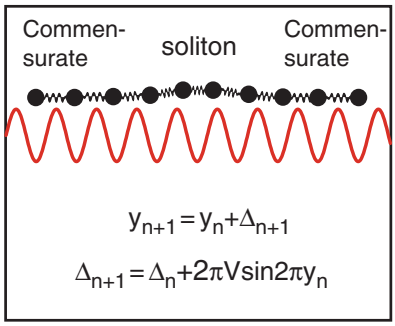


**Figure 6.** A schematic representation of the FK model. The substrate is represented by the periodic potential (red) and the ad-layer by elastically coupled ad-particles. In addition the recursion relations for the particle positions in the discrete FK model are given.

## 4. Discussion

For the c(2 × 2)-Br/Pt(110) surface the Fermi surface is located at $k_F \approx G/3$ ($G = 2.27$ Å, the reciprocal-lattice vector of the (1 × 1) surface Brillouin zone) as shown in figure 2. For $\Theta_{NO} = 0.25$ ML, $k_F \approx G/4$. The natural ad-layer period $p$ in real space scales inversely with $q = 2k_F$. Hence, in the limit of low NO coverage the natural ad-layer period $p$ should be 1.5 times the substrate period $b$. The coincidence structure therefore exhibits the actually observed threefold periodicity. Another way to see that $k_F = G/3$ results in a threefold periodicity of the combined system is by noting that $|2k_F| = 2G/3$ which, by virtue of the lattice periodicity, is equivalent to $|2G/3 - G| = G/3$. Assuming that with increasing molecular coverage the Fermi surface shrinks in a monotonic way, the period $p$ should increase continuously from 1.5 to 2. Thus, in the case of weak coupling to the substrate, one expects a succession of incommensurate and higher commensurate structures until at $q = G/2$ an ad-layer period $p = 2b$ (twofold periodicity) is obtained. Such a succession of incommensurate and higher commensurate structures is not observed. Only three commensurate structures are seen throughout the coverage range: the (3 × 1), the (7 × 1), and the (4 × 1). At intermediate coverages, which deviate from the ideal coverages associated with the three commensurate structures, the ad-layer decomposes into a mixture of the commensurate structures and randomly spaced solitons.

At this point it is necessary to consider an additional complication in the real system not discussed so far: while the periodicity of the ad-layer is governed by the position of the Fermi surface as discussed in the introduction, the ad-layer is not free to adopt its natural periodicity due to the coupling with the substrate. Thus, only in the limit of weak corrugation of the substrate potential may one expect a continuous tunability of the ad-layer periodicity. For finite substrate potential corrugation, one has to take into account the ad-layer–substrate interaction. An appropriate framework is provided in the Frenkel–Kontorova (FK) model [16]. In the following we discuss how, according to the FK model, the interaction with the substrate modifies the expected ad-layer phases as its natural periodicity is tuned from commensurate to incommensurate and back to commensurate values.

In the FK model (figure 6), the substrate is modelled as a periodic potential $V$ with period $b$. The ad-layer is represented by discrete particles. Bonding within the ad-layer is described by a harmonic force (a spring connecting the ad-particles). The natural ad-layer periodicity $p$ is given by the equilibrium positions of the ad-particles in the absence of the substrate potential. Within the discrete formulation of the FK model the ad-particle positions are determined by the recursion relations given in figure 6. Note that these relations determine only positions of force equilibrium, but not necessarily a global energy minimum.

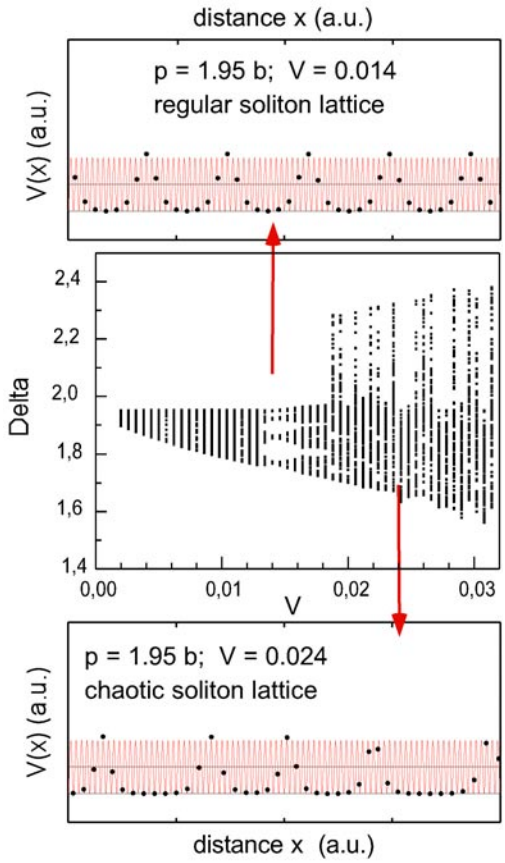


**Figure 7.** Central panel: distribution of nn distances (delta) in the ad-layer as a function of relative substrate potential $V$. A transition to chaotic behaviour occurs close to $V = 0.018$. The upper panel shows a periodic soliton lattice obtained at $V = 0.014$, the lower panel a chaotic soliton lattice obtained at $V = 0.024$. In both cases a natural overlayer periodicity of 1.95 in terms of the substrate lattice constant has been assumed. The substrate potential $V(x)$ is the periodic function shown in red. Black dots represent ad-particle positions in the substrate potential. In solitons, ad-particles are forced into unfavourable positions in the substrate potential. For the present Br/Pt(110) system the distance $x$ is measured along the $[1\bar{1}0]$ direction.

Typical traits of the FK model are illustrated in figure 7. The central panel shows a plot of nn distances occurring in the ad-layer as a function of the substrate corrugation $V$ (more precisely, $V$ is the ratio of the substrate corrugation amplitude to the spring constant $k$ characterizing the interaction between the ad-layer particles). The calculations shown here assume a natural ad-layer periodicity of $p = 1.95b$. In the limit of weak substrate corrugation the nn distances within the ad-layer converge to 1.95, which corresponds to an incommensurate, floating overlayer. The only effect of the substrate corrugation is to slightly displace the ad-particles from their natural positions, thus producing a finite spread in the ad-particle distances. Around $V = 0.014$ one observes the appearance of few well-defined nn distances. The corresponding ad-layer pattern is shown in the top panel. It consists of commensurate domains with a local twofold periodicity separated by solitons. Within the finite extent of these phase discommensurations the phase relation of the ad-layer to the substrate changes and the ad-particles are located in comparatively unfavourable positions with respect to the

substrate potential. Note, however, that the solitons are arranged periodically, yielding a so-called regular soliton lattice. This is the globally optimized solution with respect to the total energy of the system. The resulting structure is characterized by two different scales: the short-scale periodicity within the individual domains and the long-scale periodicity of the soliton lattice. In the present experiment one could interpret the $(7 \times 1)$ structure as such a regular soliton lattice. It consists of commensurate $(3 \times 1)$ domains separated from each other at periodic intervals by the NO zigzag chains. As mentioned before, the latter introduce a phase difference between the $(3 \times 1)$ domains of $2\pi/3$ ('dressed' solitons).

As the substrate potential is cranked up further, a sudden transition into chaotic behaviour takes place [16, 17]. The distribution of nn distances widens dramatically. The ad-layer relaxation into the global minimum-energy configuration becomes more and more activated. As a consequence, the ad-layer is frozen into metastable configurations corresponding to a force equilibrium but not to a global energy minimum. A typical soliton structure in this regime ($V = 0.24$) is shown in the bottom panel. Again, commensurate domains are observed, but their width varies randomly and so of course does the position of the solitons separating these anti-phase domains. Such a structure is experimentally realized for instance in figure 4(*e*). Here, the phase discommensurations are formed by bare solitons.

In figure 7 the transition from periodic to chaotic soliton lattices is illustrated as a function of substrate corrugation strength. In our experiment, however, it is not the substrate potential which is varied, but the natural periodicity $p$. At commensurate natural periodicities, periodic structures are obtained. For slight deviations from commensurability, the system tends to remain locked in a commensurate configuration (in a real system this tendency is assisted for instance by the finite terrace width of the substrate, allowing elastic relaxation at each step). At incommensurate values of $p$, however, the substrate corrugation is strong enough for the chaotic regime to be entered. Of course, the FK model in its simplified version applied here cannot be used to extract realistic figures for the parameters in the model. It serves well, however, to illustrate the basic principles giving rise to the surprisingly complex structures observed in figures 4(*b*)–(*f*).

According to the FK model, the absence of incommensurate floating layers with continuously tunable periodicity in the present experiment can be attributed to the non-negligible substrate potential (commensurability pinning). Hence, incommensurate phases are unstable and decay into commensurate domains separated by phase slips (solitons).

With respect to the interactions in the $(1\bar{1}0)$ direction it is sufficient to consider a 1D version of the FK model. Nevertheless, the present experimental situation is slightly more complicated than the FK model outlined above: the substrate potential can be identified with the corrugation provided by the Pt(110) $(1 \times 1)$ surface and the ad-layer with the Br adatoms. The positions of the latter are determined by the surface CDW. However, the NO or CO molecules used to shift the Fermi level introduce an additional complication which is not accounted for in the FK model. Up to $\Theta_{NO} = 0.14$ ML the interactions between the added molecules in the $(1\bar{1}0)$ direction can be neglected: the long-range ordering of the NO zigzag chains is obviously determined by the surface CDW and not by direct interaction of the molecules. This can be concluded from the fact that up to the $(7 \times 1)$ structure the distance between molecules in adjacent zigzag rows exceeds 8 Å. On a metallic substrate, direct adsorbate interactions are screened out on a significantly shorter length scale. Hence it is safe to assume that the long-range ordering in this structure is due to a through-substrate interaction, i.e. the charge-density oscillations. In fact, as pointed out above, the $(7 \times 1)$ structure can be considered as a regular soliton lattice. At $\Theta_{NO} = 0.11$ ML (figure 4(*b*)) the natural ad-layer periodicity is still close to $p = 1.75b$, but the NO density is not sufficient to build up a complete $(7 \times 1)$ soliton lattice. Hence, 'incomplete' dressed solitons (i.e. dressed solitons which do not extend over

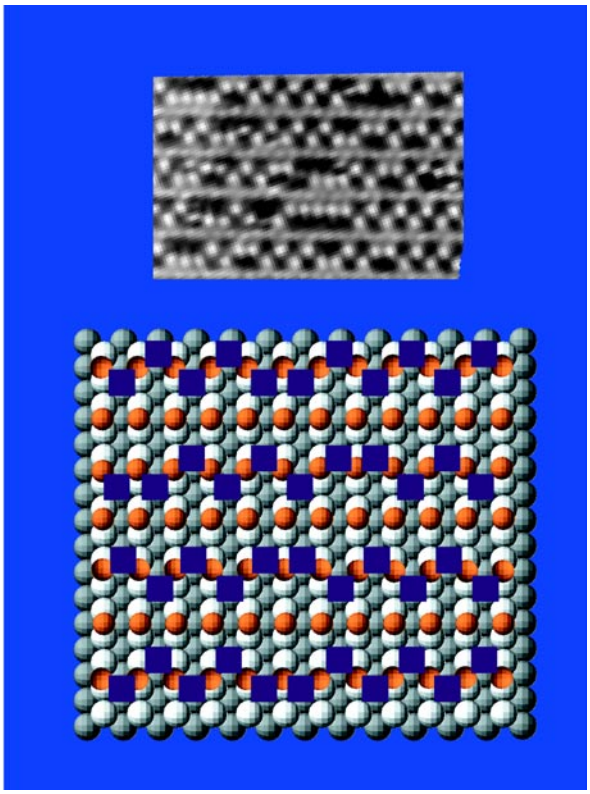

**Figure 8.** An STM image and ball model of the NO-induced $(4 \times 1)$ structure (see also figure 4(*f*)). In the ball model, Pt atoms are grey, Br atoms red and the dark blue squares symbolize the NO molecules. The Br atoms are arranged in a $(2 \times 1)$ structure.

the whole terrace) are occasionally supplemented by pairs of bare solitons which maintain the phase difference between $(3 \times 1)$ domains above and below the phase discommensuration. Close inspection of figure 4(*b*) also reveals that some of the $(3 \times 1)$ domains are broader than at $\Theta_{NO} = 0.14$ ML, because at $\Theta_{NO} = 0.11$ ML the balance is slightly tilted in favour of the $(3 \times 1)$ structure. At still lower coverage, the 1D FK model breaks down and a fluid phase is observed. Very likely the reason for this behaviour lies in the formation energy of the bare solitons: instead of forming many extended bare solitons it is energetically more favourable to introduce 'shortcuts' between incomplete dressed solitons. These 'shortcuts' are highly disordered regions, where the phase discommensuration does not run parallel to the (001) direction, thus cutting through the wavefronts of the CDW.

It remains to discuss the NO coverage range 0.25 ML $\geqslant \Theta_{NO} >$ 0.14 corresponding to a natural ad-layer periodicity $2b \geqslant p > 1.75b$. In this coverage range the direct repulsion between the NO zigzag chains, which is not part of our simple FK model, has to be taken into account as an additional factor. Thus, at $\Theta_{NO} = 0.25$ ML the NO zigzag chains have to be packed in a way which is consistent with a twofold periodicity within the Br ad-layer, yet allows for a finite distance between the NO zigzag rows. A structural model satisfying these requirements is obtained by simple extension of the vortex ball model (figure 5) and is presented in figure 8. Here, the Br atoms are arranged in a $(2 \times 1)$ structure and every second row is decorated by NO zigzag chains. The expected twofold periodicity is found in the Br ad-layer, while the NO–NO repulsion yields a fourfold periodicity in the NO sublattice.

The observed evolution from the (7 × 1) structure at $\Theta_{NO} = 0.14$ ML to the (4 × 1) structure at $\Theta_{NO} = 0.25$ ML consists in a gradual shrinking of the number of (3 × 1) domains in favour of (4 × 1) domains and the—more or less random—insertion of bare solitons (see figures 4(*d*) and (*e*)) required to obtain the average periodicity in the ad-layer determined by $q = 2k_F$. At $\Theta_{NO} = 0.23$ ML (figure 4(*e*)) the (3 × 1) domains have vanished completely, but there are still an appreciable number of randomly distributed bare solitons. These chaotic soliton structures are precisely what the FK model predicts for the case of strong substrate corrugation.

## 5. Summary

The c(2 × 2)-Br/Pt(110) adsorption system behaves as a quasi-1D surface compound. In particular it can be switched into a (3 × 1) CDW ground state by adsorption of small amounts of NO or CO. Further exposure to these molecules causes a significant change in the average ad-layer periodicity. As this change proceeds in a characteristic way already at very low adsorbate coverages, we attribute it to the variation in the CDW periodicity caused by the concomitant Fermi-surface shift. The ad-layer periodicity does not vary in a continuous fashion through commensurate and incommensurate structures, as would be expected on the basis of a continuous Fermi-surface shift. Rather, commensurate, long-range-ordered structures alternate with chaotic soliton lattices separating commensurate anti-phase domains. This is the characteristic behaviour predicted in the framework of the FK model for finite (strong) substrate corrugation. Thus making a deliberate change in the electronic structure allows one to tune the system through a succession of surprisingly complex periodic and chaotic geometries. The basic interactions involved are the natural ad-layer periodicity prescribed by $q = 2k_F$, the competition of this periodicity with the substrate periodicity and, towards higher coverages, the direct adsorbate–adsorbate interaction.

## Acknowledgments

We acknowledge essential support from the group of K Heinz (University of Erlangen) and of J Redinger (Centre of Computational Materials Science, TU Vienna). The work was sponsored by the Austrian Science Fund and the Österreichische Nationalbank.

## References

[1] Bishop A R 1997 *Synth. Met.* **86** 2203
[2] Héritier M, Pasquier C, Ravy S, Senzier P, Moradpour A and Giamarchi T (ed) 2000 *Proc. Pr3-2000 (Les Ulis): Organic Superconductivity; J. Physique* IV **10**
[3] Losio R, Altmann K N, Kirakosian A, Lin J-L, Petrovykh D Y and Himpsel FJ 2001 *Phys. Rev. Lett.* **86** 4632
[4] Carpinelli J M, Weitering H H, Plummer E W and Stumpf R 1996 *Nature* **381** 398
[5] Melechko A V, Braun J, Weitering H H and Plummer E W 1999 *Phys. Rev. Lett.* **83** 999
[6] Swamy K, Hanesch P, Sandl P and Bertel E 2000 *Surf. Sci.* **466** 11
[7] Blum V, Hammer L, Heinz K, Franchini C, Redinger J, Swamy K, Deisl C and Bertel E 2002 *Phys. Rev.* B **65** at press
[8] Swamy K, Menzel A, Beer R and Bertel E 2001 *Phys. Rev. Lett.* **86** 1299
[9] Menzel A, Beer R and Bertel E 2002 submitted
[10] Lau K H and Kohn W 1978 *Surf. Sci.* **75** 69
[11] Gumhalter B and Brenig W 1995 *Surf. Sci.* **336** 326
[12] Swamy K, Menzel A, Beer R, Deisl C, Penner S and Bertel E 2001 *Surf. Sci.* **482–5** 402
[13] Deisl C, Swamy K, Penner S and Bertel E 2001 *Phys. Chem. Chem. Phys.* **3** 1213
[14] Swamy K, Deisl C, Menzel A, Beer R, Penner S and Bertel E 2002 *Phys. Rev.* B **65** at press
[15] Marchenko V I 1992 *JETP Lett.* **55** 73
[16] Bak P 1982 *Rep. Prog. Phys.* **45** 587
[17] Aubry S 1979 *Solitons and Condensed Matter Physics* ed A R Bishop and T Schneider (Berlin: Springer) p 264